

Structure of vortices in helium at zero temperature

F. Dalfovo

Dipartimento di Fisica, Università di Trento, 38050 Povo, Italy

(Received 13 December 1991)

A density-functional theory is used to investigate the structure of vortices in superfluid helium. The angular dependence of the many-body wave function is factorized following the Feynman-Onsager hypothesis. The density profile near the vortex axis is then calculated for different values of the external pressure. The profile shows damped stationary ripples with the roton wavelength, in agreement with the predictions of previous microscopic calculations. A critical negative pressure of 8 bars is found for the stability of a vortex line against a free expansion of the core. The application of the density-functional method to the problem of ^3He impurities is also discussed.

I. INTRODUCTION

A significant part of the work done in the last decades on superfluids has been devoted to investigate quantized vortices and vortex rings (see Refs. 1 and 2 for a systematic review). While the properties of vortices on a macroscopic scale are well understood in terms of almost purely hydrodynamic models, the atomic-scale structure is still a challenging theoretical problem. The quantum-mechanical description of the vortex core and its connection with the classical macroscopic behavior are of crucial importance for the understanding of the concept of superfluidity itself. The interest in this subject is also stimulated by recent experiments which demand an accurate theory for the vortex structure. First, we mention the phase-slippage experiments by Varoquaux, Zimmermann, and Avenel,³ in which one measures the critical velocity for the flow of ^4He through small orifices. The vortex filaments and rings involved in the dissipation mechanism have such a small size that atomic-scale processes become important. Second, there are experiments which explore the behavior of liquid helium at negative pressure by means of ultrasonic waves.^{4,5} A possible mechanism invoked to explain the observed cavitation of macroscopic bubbles is the instability of vortex filaments at negative pressure, caused by the additional centrifugal energy of the superfluid flow. To predict such an instability, one has to know the pressure dependence of the vortex-core structure.

The present work is an application of the density-functional method to a rectilinear vortex. Density-functional theories are becoming more and more accurate in describing inhomogeneous phases of quantum liquids. A functional for liquid ^4He at zero temperature was introduced by Stringari and co-workers to study the free surface,⁶ helium cluster,⁷ and mixed ^3He - ^4He systems.⁸ A recent extension of that functional,^{9,10} which includes explicitly finite-range effects, has proven quite reliable in situations where short-wavelength density fluctuations play an important role. This is the case, for example, for helium films^{11,12} and the liquid-solid phase transition.¹³ In order to apply the same density functional to the case

of vortices, one has to account for the superfluid-velocity field. The simplest way is to follow the Feynman-Onsager idea,¹⁴ taking the liquid irrotational everywhere except on the axis. With this hypothesis of singular vorticity, the velocity field goes like $1/r$, where r is the distance from the axis. The velocity field acts as a centrifugal energy in the functional, generating a density profile which is necessarily zero on the axis, to avoid the divergence of the energy. In this case the present theory looks like an extension of the textbook model by Pitaevskii¹⁵ and Gross¹⁶ for vortices in weakly interacting Bose systems. It includes relevant requirements for the microscopic interaction between atoms through a quantitative consistency with the equation of state of bulk liquid, the static-response function (including the roton contribution), and the free-surface properties (profile and energy). With these ingredients the theory provides predictions for the energy and density profile of vortices at different pressures, as well as the estimate of the critical negative pressure for the instability of the vortex line.

The paper is organized as follows. In the next section we briefly review the main features of the density functional of Ref. 9 and show how it applies to the case of a rectilinear vortex. In Sec. III we present the results for the vortex structure and vortex energy at different pressures. We compare the results at zero pressure with the variational calculations of Ref. 17. We also discuss the stability of the vortex at negative pressure as well as the effect of ^3He impurities. In Sec. IV we will summarize the main results together with a few comments about future perspectives.

II. METHOD

At zero temperature the bulk liquid ^4He is completely superfluid. In terms of the two-fluid language, this means that the density of bulk liquid ^4He coincides with the superfluid density. If a vortex is present, then the superfluid winds around a line, i.e., the vortex core, with quantized circulation.¹⁴ Let us take a cylindrical frame of reference (r, θ, z) , with the z axis along the axis of a rectilinear vortex. A possible form for the N -particle wave

function is

$$\Psi(\mathbf{r}_1, \dots, \mathbf{r}_N) = \exp \left[i \sum_{j=1}^N \theta_j \right] \Phi(r_1, \dots, r_N), \quad (1)$$

where Φ is real. Such a wave function is eigenvector of the total angular momentum along z , with eigenvalue $N\hbar$. The vortex is stationary (no self-induced motion), and the associated flow has unitary circulation $\kappa = h/m$. By definition, the one-particle density is given by

$$\begin{aligned} \rho(r) &= \int d\mathbf{r}_2 \cdots d\mathbf{r}_N \Psi^*(\mathbf{r}, \mathbf{r}_2, \dots, \mathbf{r}_N) \Psi(\mathbf{r}, \mathbf{r}_2, \dots, \mathbf{r}_N) \\ &= \int d\mathbf{r}_2 \cdots d\mathbf{r}_N \Phi^2(\mathbf{r}, \mathbf{r}_2, \dots, \mathbf{r}_N). \end{aligned} \quad (2)$$

Similarly, for the current density, one has

$$\begin{aligned} \mathbf{j}(r) &= \int d\mathbf{r}_2 \cdots d\mathbf{r}_N \frac{i\hbar}{2m} [\Psi(\mathbf{r}, \mathbf{r}_2, \dots, \mathbf{r}_N) \\ &\quad \times \nabla \Psi^*(\mathbf{r}, \mathbf{r}_2, \dots, \mathbf{r}_N) - \text{c.c.}] \\ &= \hat{\theta} \frac{\hbar \rho}{mr}, \end{aligned} \quad (3)$$

having used the gradient in cylindrical coordinates and Eq. (2) for the density. The velocity field is related to the current density by the relation $\mathbf{j} = \rho \mathbf{v}$, so that

$$\mathbf{v} = \hat{\theta} \frac{\hbar}{mr}, \quad (4)$$

where $\hat{\theta}$ is a unit azimuthal vector. Expression (4) is the same as for a classical incompressible fluid. The divergence of v on the axis puts some conditions on the form of Φ . This becomes evident if one acts with the real Hamiltonian on Ψ . One has

$$\begin{aligned} H\Psi &= \left[- \sum_j \frac{\hbar^2 \nabla_j^2}{2m} + \sum_{j < k} V(|\mathbf{r}_j - \mathbf{r}_k|) \right] \Psi \\ &= \exp \left[i \sum_j \theta_j \right] \tilde{H} \Phi, \end{aligned} \quad (5)$$

where

$$\tilde{H} = H + \sum_j \frac{\hbar^2}{2mr_j^2}. \quad (6)$$

This means that Φ obeys a Schrödinger equation with an effective Hamiltonian, given by H plus a centrifugal term, coming from the velocity field. The centrifugal term implies that the wave function Φ vanishes on the axis.

This picture has been already discussed extensively in the literature. The central point is the assumption (1) for the many-body wave function. It is called the Feynman-Onsager hypothesis because those authors¹⁴ used this kind of argument to predict properties of quantized vortices in helium. In the case of a weakly interacting Bose gas, the factorization (1) is rigorously justified, and Φ^2 is identified with the amplitude of the Bose-condensate state. Thus one recovers the well-known Pitaevskii-Gross model,^{15,16} where the interaction between bosons is included via a *zero-range* repulsive potential. The density turns out to be a smooth function of r , and the size of the core is fixed by a *healing length*, which depends on the

strength of the interaction. However, liquid helium is a strongly correlated system and Φ does not coincide with the condensate wave function. Thus factorization (1) is only a reasonable way to model the superfluid density, consistent with the large-scale behavior of the quantized vortex. The more general case would be the same as Eq. (1), but with Φ a more complex function in which currents are included. This would modify the velocity field with respect to the one in Eq. (3). Since on a large scale the vortex is known to behave classically, these modifications of the velocity field would be limited to the core region. Up to now, only phenomenological theories have been proposed to account for this effect (see, for instance, Ref. 2, Chap. 4), mainly based on the two-fluid model. From the viewpoint of a more fundamental many-body theory, the validity of the Feynman-Onsager hypothesis is still an open question.

Once the angular dependence of the wave function is fixed, one is left with the problem of finding its radial dependence. The relevant quantity to be evaluated is the density $\rho(r)$, which corresponds to a static radial profile; this is equivalent to looking for the many-body wave function Φ of N atoms of ^4He in an external (centrifugal) field. The formalism we will use is that of density-functional theory, which has proven to be quite reliable for similar problems. The starting point is the idea that the total energy of a many-body system can be written as a functional of the single-particle density. The minimum of the energy is located at the true equilibrium density of the system. As the exact form of the functional is not known *a priori*, one has to choose suitable functionals, compatible with a set of basic prescriptions about symmetries and correlations in the system; in this way, one finds an approximation for the energy and density, whose quality depends on the choice of the functional. In our case the total energy E , that is, the mean value of the Hamiltonian \tilde{H} on the state Φ , is taken in the form

$$E = E_0 + \int d\mathbf{r} \frac{\hbar^2}{2mr^2} \rho, \quad (7)$$

where the second term on the right is simply the kinetic energy associated with the fluid motion around the vortex line, while E_0 is the static functional introduced in Ref. 9. The latter is given by

$$\begin{aligned} E_0 &= \int d\mathbf{r} \frac{\hbar^2}{2m} [\nabla \sqrt{\rho(r)}]^2 \\ &\quad + \frac{1}{2} \int \int d\mathbf{r} d\mathbf{r}' \rho(r) \rho(r') V(|\mathbf{r} - \mathbf{r}'|) \\ &\quad + \int d\mathbf{r} \frac{c_4}{2} \rho(r) (\bar{\rho}_r)^{1+\gamma_4}. \end{aligned} \quad (8)$$

The first term in the sum is a quantum pressure; it corresponds to the zero-temperature kinetic energy of a noninteracting Bose system. The second term contains a two-body interaction V , which is the Lennard-Jones interatomic potential,¹⁸ with the standard parameters $\alpha = 2.556 \text{ \AA}$ and $\epsilon = 10.22 \text{ K}$, screened at short distance with a power law, as follows:

$$V(x) = \begin{cases} 4\epsilon \left[\left(\frac{\alpha}{x} \right)^{12} - \left(\frac{\alpha}{x} \right)^6 \right] & \text{if } x \geq h, \\ V(h) \left(\frac{x}{h} \right)^4 & \text{if } x < h. \end{cases} \quad (9)$$

The choice of the power law is discussed in Ref. 9 and is not critical in this context. The last term accounts for short-range correlations between atoms. In particular, it contains the effect of the hard-core part of the interatomic potential. Its form follows the idea of the "weighted-density approximation," used mainly in the study of classical fluids. The weighted density $\bar{\rho}$ is

$$\bar{\rho}_r = \int d\mathbf{r}' \rho(\mathbf{r}') \Pi_h(|\mathbf{r}-\mathbf{r}'|), \quad (10)$$

with

$$\Pi_h(x) = \begin{cases} 3(4\pi h^3)^{-1} & \text{if } x < h, \\ 0 & \text{if } x \geq h. \end{cases} \quad (11)$$

The parameters c_4 and γ_4 , together with the screening length h , are the only three parameters of the theory; they are fixed to reproduce the equation of state of the bulk liquid. Their values are given in Table I. As discussed in Ref. 9, the functional E_0 corresponds to a mean-field description, which incorporates phenomenologically the effects of a finite-range interaction, with the correct long-range behavior and inclusion of short-range correlations. The relevant features of the functional E_0 in this context are (a) it gives the equation of state also at negative pressure, predicting a vanishing sound velocity, i.e., the mechanical instability of the liquid, at -9 bars; (b) it yields a static-response function (polarizability), in agreement with the experimental data, available at zero pressure, accounting correctly for the effect of the phonon-roton excitations; (c) it gives a smooth free-surface profile, 6 \AA thick, and with surface tension very close to the experimental one; (d) it accounts for localization effects, such as the density fluctuations near a molecular or ionic impurity,¹⁰ the layer structure of helium films,^{11,12} and the solidification at high pressure;¹³ and (e) it is easily generalized to include the effect of ^3He impurities.^{8,11}

The total energy (7) has the functional form

$$E = \int d\mathbf{r} \mathcal{H}[\rho(r)], \quad (12)$$

which has to be minimized with respect to ρ to get the density profile around the vortex line. The corresponding Euler-Lagrange equation is

$$\left[-\frac{\hbar^2}{2m} \frac{1}{r} \frac{d}{dr} r \frac{d}{dr} + \frac{\hbar^2}{2mr^2} + U(r) \right] \sqrt{\rho} = \mu \sqrt{\rho}, \quad (13)$$

TABLE I. Parameters entering functional (12).

γ_4	2.8
h_4	2.3767 \AA
c_4	$10\,455\,400 \text{ K \AA}^{3(1+\gamma_4)}$

where

$$U(r) = \int d\mathbf{r}' \rho(\mathbf{r}') V(|\mathbf{r}-\mathbf{r}'|) + \frac{c_4}{2} \bar{\rho}_r^{1+\gamma_4} + \frac{c_4}{2} (1+\gamma_4) \int d\mathbf{r}' \Pi_h(|\mathbf{r}-\mathbf{r}'|) \rho(\mathbf{r}') \bar{\rho}_r^{\gamma_4}. \quad (14)$$

Equation (13) can be solved numerically by using the so called *imaginary-time-step* method, as done in Ref. 9 for the free surface. The geometry, with a mixing of cylindrical and spherical symmetries makes the calculation a little more complicated. The pressure P is simply included in the theory by imposing the proper limiting value for the density far from the vortex. The density for large r must approach the bulk-liquid density at a given pressure, and μ will correspond to the chemical potential at the same pressure. Once the density profile is found, the energy per unit length of the vortex is given by

$$E_v = 2\pi \int dr [\mathcal{H}(r) - \mu \rho(r) + P]. \quad (15)$$

Finally, we note that the Pitaevskii-Gross model for the vortex is formally included in Eq. (13). It is sufficient to consider only a zero-range repulsive force between particles, having strength U_0 . In such a way, the potential U of Eq. (14) would be replaced by a term $U_0 \rho$, and Eq. (15) would take the same form of the Pitaevskii equation for the vortex profile.

III. RESULTS

A. Vortex structure

Solving Eq. (13) at zero temperature, one finds the density profile shown in Fig. 1. The calculation is done in a cylinder of given radius R , much bigger than the expected core radius, and the density at the boundary is taken to be the bulk-liquid density. The resulting vortex energy per unit length increases logarithmically with R . This follows from the centrifugal energy term, in $1/r$, con-

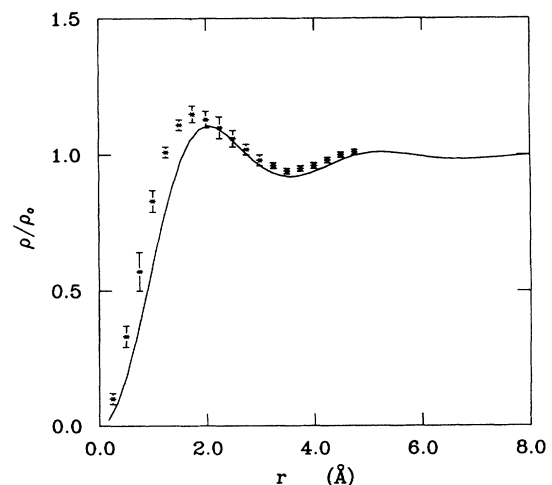


FIG. 1. Density profile for a vortex at zero pressure and zero temperature. The solid line is the result of the present work. The points with error bars are the results of Ref. 17. The bulk-liquid density is $\rho_0 = 0.0218 \text{ \AA}^{-3}$.

tained in \mathcal{H} . The remaining part of the integrand in Eq. (15) is nonzero only near the vortex core and vanishes when the density reaches the value of the bulk liquid, i.e., at distances of the order of 10 \AA from the axis. The profile in Fig. 1 is evaluated with a cutoff radius of $R = 17 \text{ \AA}$, and the corresponding energy turns out to be $E_v = 3.0 \text{ K/\AA}$. For comparison in the same figure, we show the density profile obtained in Ref. 17 with variational calculations, the error bars accounting for different parametrizations of the wave function. The energy of the vortex given by the two theories is of the same order. In particular, choosing the same cutoff radius of 6 \AA we find an energy of 2 K/\AA , while in Ref. 17 the energy is found in the range $2.3\text{--}2.8 \text{ K/\AA}$.

The core size, i.e., the radius of the region where the density drops to zero, is of the order of 1 \AA ; this is a typical size coming out in any theory subject to the Feynman-Onsager ansatz for the velocity field and consistent with a minimal set of physical requirements (compressibility, surface tension, etc.). A more qualifying feature is the oscillating behavior of the density outside the core. These oscillations can be easily fitted with a sum of a monotonic function, which starts as r^2 near the axis and approaches asymptotically the bulk density at large r , and a damped Bessel function $J_0(qr)$, where q is the wave vector of rotons. The connection between the spectrum of elementary excitations in ^4He and the density profile near a boundary was established theoretically by Regge and Rasetti.¹⁹ They considered the boundary as a localized *source* of elementary excitations. In the limit of small perturbations, they found an expression for the density in terms of the static-response function. The main effect comes from the part of the spectrum near the roton minimum, and the profile shows permanent ripples, having the roton wavelength and an amplitude which decreases exponentially in the bulk liquid. Their analysis was applied to the case of a free surface and to helium droplets. In those cases, however, the diffuseness of the surface itself (having a thickness of the order of $6\text{--}10 \text{ \AA}$) makes the hypothesis of localized source not valid and the ripples are washed out. The case of a vortex is more favorable since the vortex core is localized in a radius of about 1 \AA , and the hypothesis of Regge and Rasetti works well. From another viewpoint one can interpret the density oscillations as the tendency of the liquid to organize itself in shells of atoms around the vortex line, as well as in the vicinity of any localized *impurity*. This rearrangement does not require much energy if the interatomic distance is unchanged. The effect is formally included in the theory if the latter accounts properly for the linear-response function, which is peaked at the roton wavelength. It is worth noting that the presence of density oscillations should not depend strictly on the ansatz for the velocity field in the core region. Furthermore, we point out that in the classical picture for a vortex these oscillations do not appear. If one writes down the classical hydrodynamic equations, one finds a density which decreases monotonically from the bulk toward the vortex core. The classical picture has been often used to extract information from experimental data, and the role of possible density oscillations has never been discussed.

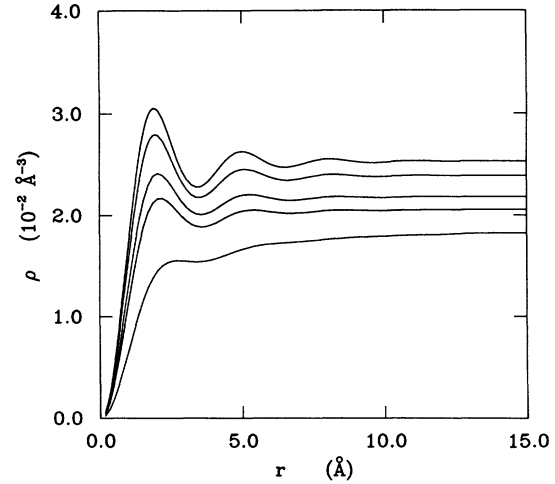


FIG. 2. Density profile for a vortex for different values of the external pressure. Starting from the upper curve, the pressure is taken to be 20, 10, 0, -4 , and -8 bars. The lowest curve corresponds to the last stable vortex.

B. Pressure dependence

A striking feature of the density functional is that the pressure dependence of all quantities is derived straightforwardly. We solved the equation for the density profile around the vortex line as a function of pressure. The resulting profiles are shown in Fig. 2. The qualitative form is the same: a monotonic $\rho(r)$, which goes as r^2 near the axis, superimposed by oscillations. The wavelength of such ripples corresponds almost exactly to the roton wavelength at each pressure. At negative pressures the oscillations are less and less pronounced, which means that the atoms have less tendency to localize.

An important result is that below -8 bars the vortex turns out to be mechanically unstable. From the numerical viewpoint, the instability of the vortex appears as a lack of convergence in the iterative procedure. At each step the density profile moves slowly away from the axis; i.e., the core size becomes larger and larger. The typical situation is shown in Fig. 3, where the energy E_v is plotted as a function of the iteration number. The solid lines correspond to several runs, each one at a different pressure, in which the starting density profile is chosen to have a core radius slightly smaller than the expected one. The dashed lines are runs, at the same values of pressure, in which the initial core radius is larger than the expected one. Each curve takes $3\text{--}6$ h of CPU time on a VAX-60320, depending on the choice for the cutoff radius and spatial step. At any given pressure, the calculation converges to a stable solution, independently of the initial input. However, the convergence is slower and slower approaching -8 bars. For pressure less than -8 bars, we do not find convergence; i.e., the energy E_v decreases indefinitely.

From a physical viewpoint, one can understand this effect qualitatively by considering the simple hollow core model, with a sharp density profile. A negative external pressure favors the expansion of the core radius, through a negative Gibbs-free-energy term proportional

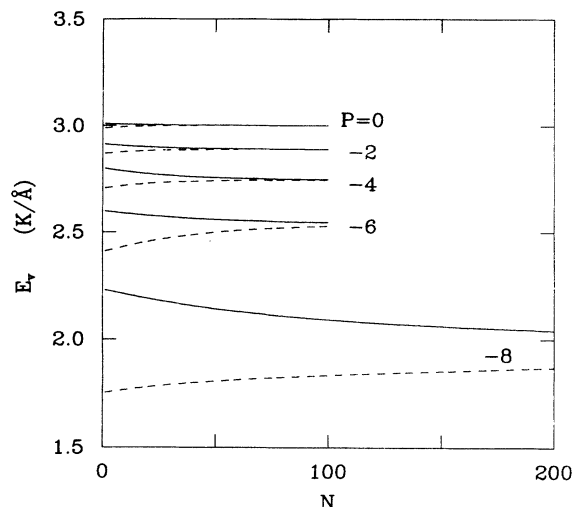


FIG. 3. Vortex energy per unit length as a function of the iteration number and for several pressures (in bars). Solid and dashed lines correspond to different choices for the initial density profile (see text).

to the volume of the hollow core; this term is counterbalanced by the surface free energy, which is positive and proportional to the surface area. The total free energy, including the centrifugal energy of the fluid flow, will have a minimum at a given radius, as well as an energy barrier against the spontaneous expansion of the core. This will be true only down to a critical value of P at which the barrier height is zero. For pressure more negative than the critical one, the vortex gains energy by expansion of the core. Though this model is not quantitative (it gives a core size of 0.5 \AA at zero pressure, while the surface energy is taken equal to the one of a free surface, which is much thicker), it gives correct hints about the real situation.

The investigation of the vortex structure at negative pressure is motivated by recent experiments,^{4,5} in which negative pressures are produced by focusing ultrasonic waves in a sample of bulk-liquid helium. The local fluid velocity in the sample allows the creation of vortices. The pressure (tensile strength) at which the phenomenon of cavitation occurs, by nucleation of bubbles, could be influenced significantly by the presence of vortices, changing the interpretation of the experimental data. The existence of a critical pressure for the vortex stability puts an upper bound for the tensile strength. An estimate for such a pressure has been already given in Xiong and Maris.⁵ They give a value of -6.5 bars to be compared with our -8 bars. Both estimates comes out from density-functional calculations. In Ref. 5 the density functional is local and includes nonlocal effects in the free-energy density through a term proportional to the gradient squared of the density, $\lambda(\nabla\rho)^2$. Apart from minor differences, this is equivalent to a local approximation (or a gradient expansion) of the functional (12). The two functionals are expected to give similar results when the density does not change too fast, i.e., in the case of the free surface or bubbles. In the vortex case, the system is inhomogeneous on a shorter length scale, so that the

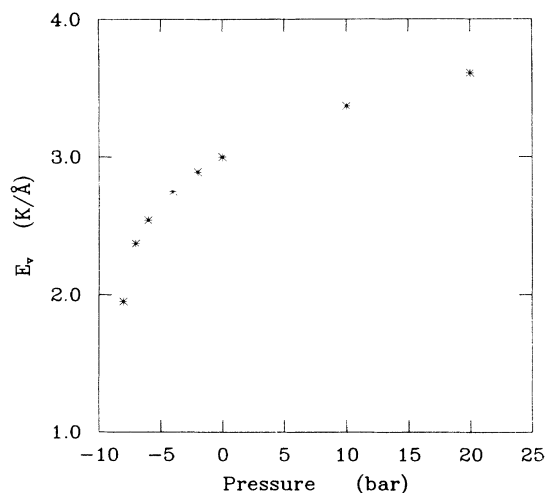


FIG. 4. Vortex energy calculated with a cutoff radius of 17 \AA for several values of the external pressure.

functional (12) is expected to be more quantitative. In particular, a functional with a $(\nabla\rho)^2$ term does not account for localization effects (ripples), yielding slightly less stable vortices than the functional (12).

Finally, we discuss the behavior of the vortex energy with pressure. In Fig. 4 we show our results for the vortex energy at different pressures, for a cutoff radius of 17 \AA . The energy increases smoothly for positive pressures, while it lowers abruptly near -8 bars. We remember that the kinetic energy associated with the fluid flow diverges logarithmically when the radius goes to infinity, because the velocity goes as $1/r$ and the density is almost the bulk density. We point out that from a knowledge of the energy one cannot extract unequivocally the so-called *core parameter* a . The latter enters the following parametrization for the energy:

$$E_v = \frac{\rho_0 \kappa^2}{4\pi} \left[\ln \left[\frac{R}{a} \right] + \delta \right], \quad (16)$$

where $\kappa = h/m$ is the quantum of circulation, ρ_0 is the bulk density, and δ is another parameter related to the structure of the core. An equivalent parametrization has been used for the energy and velocity of vortex rings. The analysis of the experimental data on vortex rings in terms of the core parameter depends on the choice for δ .²⁰ This is related to the “rigidity” of the vortex core, i.e., the potential energy in the core region. Different values are extracted if the core is taken as an hollow core or a rigid rotating cylinder. This makes it impossible to compare directly our results for the energy with available tabulations of the core parameter as a function of pressure.^{2,20} The latter are derived assuming a pressure-independent δ , while our results suggest that the *rigidity* of the vortex can change significantly with pressure.

C. ³He impurities

³He impurities in bulk ⁴He can be seen as microscopic probes for the structure of vortices. They tend to be localized along the vortex as a consequence of quantum

correlations. The effects of this binding are experimentally accessible.^{21,22} Several theories have been developed to explain the interaction between ^4He vortices and ^3He atoms.^{23–26} There are two main contributions to the energy of one ^3He atom, which have to be properly accounted for: a *kinematic* energy associated with the presence of a superfluid flow and a *mean-field* energy $\epsilon(\rho)$ independent of v_s . The first one requires some assumptions on the effective mass of the ^3He atom. The second one has been so far included only in a semiquantitative way, using a classical Bernoulli pressure drop as input.²⁶ All estimates agree with a binding energy of the order of 3 K for the vortex state referred to the bulk state. Here we want to show that the role of $\epsilon(\rho)$ is important and that it can be worked out by means of the density-functional method. The functional in Sec. II has been already generalized to study ^3He impurities on ^4He films.¹¹ The idea is to add few more terms which depend on the ^3He density, with the corresponding parameters fixed to reproduce known properties of ^3He - ^4He mixtures (the binding energy in the uniform system and excess-volume parameter). The minimization with respect to the ^3He density provides a Schrödinger-like equation. The important point is that a local depletion of the ^4He density produces a potential well for the wave function of the ^3He atom. This is true also for vortices. Using the profile in Fig. 1 as input in the formalism of Ref. 11, one finds a potential well for ^3He , centered on the vortex axis and with a depth of about 6 K with respect to energy of one ^3He atom in bulk ^4He . If the mass of the ^3He atom is taken to be equal to the bare atomic mass, the binding energy for ^3He in the core turns out to be -2.7 K. This result gives an order of magnitude for the effect of $\epsilon(\rho)$. It suggests that, if the density profile of a vortex is as in Fig. 1, then (a) the effect of the ^4He density on ^3He atoms cannot be simulated simply by a Bernoulli pressure drop and (b) the attraction caused by the density depletion near the core is comparable with the one induced by the superfluid flow.

IV. CONCLUSIONS

We have presented a calculation for the structure of a vortex in superfluid ^4He in the limit of zero temperature. The framework is the one of density-functional theories. In particular, we started by noting that a very accurate functional is now available⁹ to study inhomogeneous states of helium, such as surfaces, clusters, films, and im-

purities. In order to apply the same functional to the case of a rectilinear vortex, we took the Feynman-Onsager form for the superfluid-velocity field; i.e., we factorized the angular dependence of the N -body wave function as in Eq. (1). With this choice the calculation for the radial density profile is easily performed at any given external pressure. The main results are as follows.

(i) At zero pressure the density profile is in agreement with the one obtained with previous variational calculations,¹⁷ where the same ansatz for the velocity field was used. The core size is of the order of 1 Å, and the density profile shows permanent ripples. The wavelength and damping of such oscillations are in agreement with theoretical arguments by Regge and Rasetti¹⁹ and confirm the accuracy of the density functional on the atomic-length scale.

(ii) If the external pressure increases, the core size becomes slightly smaller and the amplitude of the ripples grows. However, at negative pressure, the profile is smoother and smoother, until a critical pressure of -8 bars; below this value, the vortex line becomes unstable against a free expansion of the core. We have discussed this instability in the context of ultrasonic experiments on helium at negative pressure.^{4,5}

(iii) The density functional can be extended to include the effect of ^3He impurities. We have shown that the role of the ^4He density profile is important in determining the binding energy for ^3He atoms on the vortex line.

These results represent an application of density-functional methods to vortices. Further work is in progress in two main directions. First, we can apply the same formalism to predict the structure of vortex rings. This implies only a change of geometry and more care in the optimization of the numerical procedure. Second, we are exploring the generalization of the density functional beyond the Feynman-Onsager approximation. A natural way would consist of adding terms which depend explicitly on the current density. A density functional accounting for current-current correlations could produce a distributed vorticity and a nonzero density in the core.

ACKNOWLEDGMENTS

I am indebted to R. M. Bowley, L. Pitaevskii, and S. Stringari for many useful discussions. This work was partially supported by INFN, gruppo collegato di Trento.

¹A. L. Fetter, in *The Physics of Liquid and Solid Helium*, edited by K. H. Bennemann and J. B. Ketterson (Wiley, New York 1976), Pt. I, Chap. 3.

²R. J. Donnelly, *Quantized Vortices in Helium II*, Cambridge Studies in Low Temperature Physics (Cambridge University Press, Cambridge, England, 1991).

³E. Varoquaux, W. Zimmermann, and O. Avenel, in *Excitations in Two-Dimensional and Three-Dimensional Quantum Fluids*, edited by A. G. F. Wyatt and H. J. Lauter (Plenum, New York, 1991), p. 343.

⁴J. A. Nissen, E. Bodegom, and J. S. Semura, *Phys. Rev. B* **40**, 6617 (1989).

⁵H. J. Maris and Q. Xiong, *Phys. Rev. Lett.* **63**, 1078 (1989); Q. Xiong and H. J. Maris, *J. Low Temp. Phys.* **77**, 347 (1989); **82**, 105 (1991).

⁶S. Stringari and J. Treiner, *Phys. Rev. B* **36**, 8369 (1987).

⁷S. Stringari and J. Treiner, *J. Chem. Phys.* **87**, 5021 (1987).

⁸F. Dalfovo and S. Stringari, *Phys. Lett.* **112A**, 171 (1985); *Phys. Scr.* **38**, 204 (1988); F. Dalfovo, *Z. Phys. D* **14**, 263 (1989).

⁹J. Dupont-Roc, M. Himbert, N. Pavloff, and J. Treiner, *J. Low Temp. Phys.* **81**, 31 (1990).

¹⁰N. Pavloff, thesis, Orsay, Université de Paris-Sud, 1990.

¹¹N. Pavloff and J. Treiner, *J. Low Temp. Phys.* **83**, 331 (1991).

¹²E. Cheng, M. W. Cole, W. F. Saam, and J. Treiner, *Phys. Rev.*

- Lett. **67**, 1007 (1991).
- ¹³F. Dalfovo, J. Dupont-Roc, N. Pavloff, S. Stringari, and J. Treiner, *Europhys. Lett.* **16**, 205 (1991).
- ¹⁴L. Onsager, *Nuovo Cimento Suppl.* **6**, 249 (1949) (discussion on paper by C. J. Gorter); R. P. Feynman, in *Progress in Low Temperature Physics*, edited by C. J. Gorter (North-Holland, Amsterdam, 1955), Vol. I, Chap 2.
- ¹⁵L. P. Pitaevskii *Zh. Eksp. Teor. Fiz.* **40**, 646 (1961) [*Sov. Phys. JETP* **13**, 451 (1961)].
- ¹⁶E. P. Gross, *Nuovo Cimento* **20**, 454 (1961).
- ¹⁷G. V. Chester, R. Metz, and L. Reatto, *Phys. Rev.* **175**, 275 (1968).
- ¹⁸The choice of the Lennard-Jones, instead of more accurate interatomic potentials (such as the Aziz potential), is a matter of convenience. The essential point is the inclusion of a correct long-range behavior. Then the density functional is tuned to reproduce bulk properties of liquid helium.
- ¹⁹T. Regge, *J. Low Temp. Phys.* **9**, 123 (1972); M. Rasetti and T. Regge, in *Quantum Liquids*, edited by J. Ruvalds and T. Regge (North-Holland, Amsterdam, 1978), p. 227.
- ²⁰W. I. Glaberson and R. J. Donnelly, in *Progress in Low Temperature Physics*, edited by D. F. Brewer (North-Holland, Amsterdam, 1966), Vol. IX, Chap. 1.
- ²¹R. M. Ostermeier, E. J. Yarmchuk, and W. I. Glaberson, *Phys. Rev. Lett.* **35**, 957 (1975); R. M. Ostermeier and W. I. Glaberson, *J. Low Temp. Phys.* **25**, 317 (1976).
- ²²G. A. Williams and R. E. Packard, *J. Low Temp. Phys.* **33**, 459 (1978).
- ²³L. S. Rent and I. Z. Fischer, *Zh. Eksp. Teor. Fiz.* **55**, 722 (1968) [*Sov. Phys. JETP* **28**, 375 (1969)].
- ²⁴T. Ohmi, T. Tsuneto, and T. Usui, *Prog. Theor. Phys.* **41**, 1395 (1969); T. Ohmi and T. Usui, *ibid.* **41**, 1400 (1969).
- ²⁵M. Kuchnir, J. B. Ketterson, and P. R. Roach, *Phys. Rev. A* **6**, 341 (1972).
- ²⁶C. M. Muirhead, W. F. Vinen, and R. J. Donnelly, *Proc. R. Soc. London A* **402**, 225 (1985).